Hindawi Publishing Corporation
EURASIP Journal on Wireless Communications and Networking
Volume 2009, Article ID 293264, 8 pages
doi:10.1155/2009/293264

Research Article

BER Degradation of MC-CDMA at High SNR with MMSE Equalization and Residual Frequency Offset

P. Harinath Reddy and V. U. Reddy

International Institute of Information Technology, Hyderabad, India

Correspondence should be addressed to V. U. Reddy, vur@iiit.ac.in

Received 19 May 2009; Revised 27 October 2009; Accepted 15 December 2009

Recommended by Wolfgang Gerstacker

Multicarrier Code Division Multiple Access (MC-CDMA) is an attractive technique for high speed wireless data transmission in view of its advantages over orthogonal frequency division multiplexing. In this paper, we analyze the performance of fully loaded downlink MC-CDMA systems with minimum mean square error (MMSE) equalizer in the presence of residual frequency offset (RFO) in multipath Rayleigh fading channels. We first show that as the SNR is increased beyond a value, referred as threshold SNR, the performance degrades. We then analyze the cause for this behavior and propose a remedy to prevent the degradation by regularizing the coefficient(s) of the equalizer, and use the regularized equalizer for SNRs beyond the threshold value. We suggest two methods for estimating this SNR, one gives close to the true value but requires the knowledge of RFO and the channel state information (CSI), while the other gives an approximate value but requires only CSI. We show that the regularization based on the approximate value also prevents the degradation, but the performance at higher SNRs is slightly poorer compared to that with the better estimate. Numerical and simulation results are provided to support the analysis.

1. Introduction

Orthogonal Frequency Division Multiplexing (OFDM) employs a number of orthogonal subcarriers to transmit symbols in parallel. This increases the symbol duration which aids in combating multipath interference. Although OFDM is attractive for high-speed wireless data transmission, it suffers from lack of frequency diversity. Spreading along the subcarriers introduces the frequency diversity and this is implemented in Multicarrier Code Division Multiple Access (MC-CDMA) system. Combination of frequency diversity and an appropriate equalizer yields improved bit error rate (BER) performance in multipath channels compared to OFDM [1].

In OFDM systems, timing and frequency synchronization is very important [2]. In particular, lack of frequency synchronization causes loss of orthogonality among the subcarriers thereby introducing the inter carrier interference (ICI). Though several algorithms are proposed for estimating and correcting the frequency offset [3, 4], there will always be some amount of residual frequency offset (RFO) left uncompensated. In [5], the authors analyze the BER performance of the OFDM in multipath fading channels in the presence of RFO.

As MC-CDMA is a combination of OFDM and CDMA, it is sensitive to RFO [6–8]. In [6, 7], the authors analyzed the performance of MC-CDMA in the presence of RFO using equal gain combining and maximal ratio combining equalizers. In [8], the authors discussed the sensitivity of two-dimensional spreading schemes, such as orthogonal frequency code division multiplexing, to synchronization errors using zero-forcing (ZF) and minimum mean square error (MMSE) equalizers.

In this paper, we analyze the performance of fully loaded downlink MC-CDMA in the presence of RFO with ZF and MMSE equalizers. In particular, we obtain a closed-form expression for the average signal-to-interference-plus noise ratio (SINR) at the output of despreader. We then show that though the performance of the MMSE equalizer is significantly better than that of ZF at lower SNRs, it

starts degrading beyond a SNR value, referred hereafter as threshold SNR, which depends on RFO and the profile of multipath channel, and tends towards that of ZF as SNR is increased further. We analyze the cause for this behavior and suggest a remedy to prevent degradation by regularization of the coefficient(s) of the MMSE equalizer. The regularized equalizer is used for SNRs beyond the threshold value. We suggest two methods for estimating this SNR value, one of them gives close to the true value but it requires the knowledge of RFO and channel state information (CSI), while the other gives an approximate value which needs only CSI. If the actual value of RFO is less than the assumed, the threshold SNR estimated based on the assumed RFO will still be appropriate. The regularization with approximate value of the threshold SNR also prevents degradation, but with a small loss in the BER performance at higher SNRs compared to that with the better estimate. Numerical and simulation results are provided to support the analysis.

The rest of the paper is organized as follows. Section 2 provides a brief background of an MC-CDMA system. In Section 3, we introduce the received signal model at the FFT output in the presence of RFO. In Section 4, we obtain the expression for BER with MMSE and ZF equalizers and bring out the degradation with the former at high SNRs. In Section 5, we analyze the cause for the degradation beyond a threshold SNR and suggest a remedy as well as two methods for estimating the threshold SNR. Section 6 gives simulation results for multipath Rayleigh fading channels, and Section 7 concludes the paper.

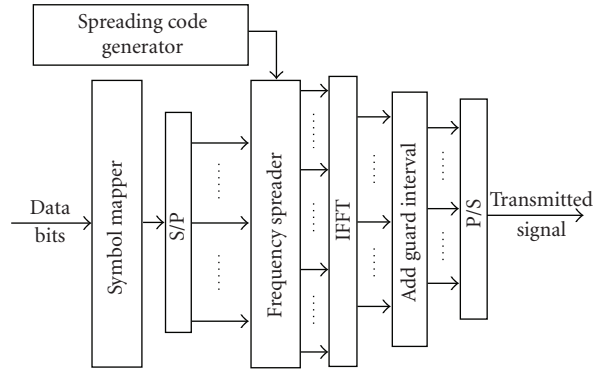

Figure 1: Transmitter of an MC-CDMA system.

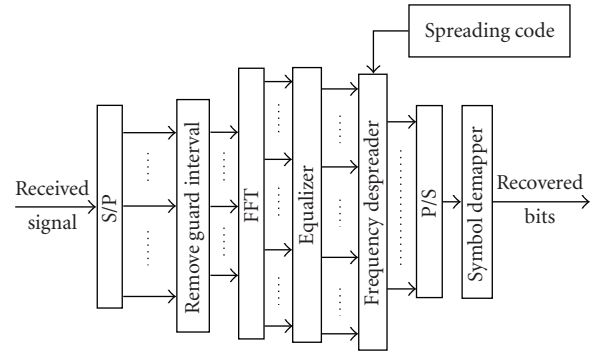

Figure 2: Receiver of an MC-CDMA system.

2. Brief Background of an MC-CDMA System

In MC-CDMA, the spreading is implemented in frequency. Here, we use Walsh-Hadamard codes for spreading. For convenience, we assume that the frequency spreading factor is same as the number of subcarriers, N_f, which is an integer power of 2. Let $\mathbf{W}^{N_f}$ denote the Walsh-Hadamard matrix of size $N_f \times N_f$:

$$\mathbf{W}^{N_f} = \left[\mathbf{w}_0^{N_f} \quad \mathbf{w}_1^{N_f} \quad \cdots \quad \mathbf{w}_{N_f-1}^{N_f}\right], \tag{1}$$

where $\mathbf{w}_k^{N_f} = [w_{0,k}^{N_f} \quad w_{1,k}^{N_f} \quad \cdots \quad w_{N_f-1,k}^{N_f}]^T$ with the superscript T denoting transpose of a vector.

Let the symbols be a_k, $0 \le k \le N_f - 1$. The symbol a_k is spreaded in frequency by $\mathbf{w}_k^{N_f}$. The output of the frequency spreader block (see Figure 1) is given by

$$\mathbf{x} = \sum_{k=0}^{N_f-1} \mathbf{w}_k^{N_f} a_k, \tag{2}$$

where $\mathbf{x}$ is a vector of size $N_f \times 1$. From the above equation it is clear that we are considering a fully loaded downlink MC-CDMA system. The output of this block is fed to the IFFT block whose output is given by

$$\mathbf{y} = \mathbf{F}\mathbf{x}, \tag{3}$$

where $\mathbf{y} = [y_0 \quad y_1 \quad \cdots \quad y_{N_f-1}]^T$ and $\mathbf{F}$ denotes normalized IFFT matrix. The output $\mathbf{y}$ is sent to the Add Guard Interval block where the cyclic prefix of length $(L-1)$ is added giving

$$\tilde{\mathbf{y}} = \left[y_{N_f-L+1} \quad y_{N_f-L} \quad \cdots \quad y_{N_f-1} y_0 \quad \cdots \quad y_{N_f-1}\right]^T_{(N_f+L-1)\times 1}, \tag{4}$$

and $\tilde{\mathbf{y}}$ is transmitted after parallel to serial conversion.

The receiver block diagram is shown in Figure 2. The received signal is first passed through a serial to parallel converter and then given to the FFT block after removing the guard interval (cyclic prefix). The output of the FFT block is fed to equalizer block and its output is given to the frequency despreader block. The other blocks are parallel to serial converter and symbol demapper (see Figure 2).

3. Received Signal Model at the FFT Output in the Presence of RFO

At the receiver, we perform timing and frequency synchronization and channel estimation using a preamble. We assume perfect timing synchronization and perfect knowledge of the CSI. Also, we assume that some amount of RFO will be left after correction with estimated carrier frequency offset, and normalized value of this (normalized with subcarrier spacing) is of the order 10^{-2}. Let this RFO be denoted by ϵ.

We collect $(N_f + L - 1)$ samples of the received signal, remove the cyclic prefix, and compute its FFT. The FFT output is given by

$$\mathbf{r} = e^{i2\pi\epsilon(n(N_f+L-1)+L-1)/N_f}\mathbf{F}^H\mathbf{T}\mathbf{H}\mathbf{y} + \eta, \tag{5}$$

where the superscript H denotes Hermitian transpose, n refers to nth MC-CDMA symbol and the exponent is the phase accumulation term after removing cyclic prefix. $\mathbf{H}$ is a circulant matrix:

$$\mathbf{H} = \begin{bmatrix} h_0 & 0 & \cdots & h_{L-1} & h_{L-2} & \cdots & h_1 \\ h_1 & h_0 & \cdots & 0 & h_{L-1} & \cdots & h_2 \\ \vdots & \vdots & \ddots & \ddots & \ddots & \ddots & \vdots \\ h_{L-2} & h_{L-3} & \cdots & h_0 & 0 & \cdots & h_{L-1} \\ h_{L-1} & h_{L-2} & \cdots & h_1 & h_0 & \cdots & 0 \\ \vdots & \vdots & \ddots & \ddots & \ddots & \ddots & \vdots \\ 0 & 0 & \cdots & h_{L-1} & h_{L-2} & \cdots & h_0 \end{bmatrix}_{N_f \times N_f}, \tag{6}$$

and $\mathbf{T}$ is

$$\mathbf{T} = \text{diag}\left[1 \; e^{(i2\pi\in/N_f)} \; \cdots \; e^{(i2\pi\in(N_f-1)/N_f)}\right], \tag{7}$$

where diag$[\cdot]$ denotes a diagonal matrix with the elements as its diagonal elements, and $i = \sqrt{-1}$. η is a circularly symmetric complex Gaussian noise vector of size $N_f \times 1$ with independent and identically distributed elements, each having zero mean and variance σ^2. In (6), $h_0, h_1, \ldots, h_{L-1}$ are the L channel impulse response coefficients, each of which is modeled as a complex Gaussian variable with zero mean and variance $\sigma^2_{h_i}$, $i = 0, 1, \ldots, L-1$, and we assume that they are mutually uncorrelated.

From [5], (5) can be written as

$$\mathbf{r} = e^{i2\pi\epsilon(n(N_f+L-1)+L-1)/N_f}e^{i\pi\epsilon(N_f-1)/N_f}\overline{\mathbf{T}}\mathbf{\Lambda}\mathbf{x} + \eta, \tag{8}$$

where (m,l)th element of $\overline{\mathbf{T}}$, for $m, l = 0, 1, \ldots, N_f - 1$, is

$$\overline{\mathbf{T}}(m,l) = \frac{\sin(\pi((l-m)+\epsilon))}{N_f \sin\left(\pi((l-m)+\epsilon)/N_f\right)} e^{i\pi(N_f-1)((l-m))/N_f}, \tag{9}$$

and $\mathbf{\Lambda}$ is a diagonal matrix with the diagonal elements as the eigenvalues of $\mathbf{H}$. Let these eigenvalues be $\lambda_0, \lambda_1 \cdots \lambda_{N_f-1}$. They represent the subchannel (bin) gains. We may point out here that the N_f DFT coefficients of $h_0, h_1, \ldots, h_{L-1}$, computed using the normalized DFT and scaled by $\sqrt{N_f}$, represent the eigenvalues of $\mathbf{H}$.

The term $e^{i2\pi\epsilon(n(N_f+L-1)+L-1+(N_f-1)/2)/N_f}$ in (8) is the common phase error and we assume that the receiver is able to perfectly compensate this error for each block using pilot tones (see [5, 9]). After compensation with common phase error, we have

$$\widetilde{\mathbf{r}} = \overline{\mathbf{T}}\mathbf{\Lambda}\mathbf{x} + \widetilde{\eta}, \tag{10}$$

In view of the model assumed for η, the elements of $\widetilde{\eta}$ are also i.i.d complex Gaussian with zero mean and variance σ^2.

4. BER Performance of MC-CDMA with MMSE and ZF Equalizers in the Presence of RFO

Note that frequency selective nature of the multipath channel causes multicode interference (MCI) while RFO causes intercarrier interference (ICI). If the value of RFO is known as well as the knowledge of CSI, we can design the equalizer to combat both MCI and ICI. However, in practice, we will not have the knowledge of the exact value of RFO, and hence, we design the equalizer only to combat MCI.

Let $\mathbf{V}_{\text{eq}}$ denote the equalizer matrix. Applying this to the signal (10), we have

$$\mathbf{d} = \mathbf{V}_{\text{eq}}\widetilde{\mathbf{r}} = \sum_{l=0}^{N_f-1} a_l \mathbf{V}_{\text{eq}}\overline{\mathbf{T}}\mathbf{\Lambda}\mathbf{w}_l^{N_f} + \mathbf{V}_{\text{eq}}\widetilde{\eta}, \tag{11}$$

where we replaced $\mathbf{x}$ with (2), and $\mathbf{d}$ is a vector of size $N_f \times 1$. Next, we apply frequency despreading to decode the transmitted symbol a_m :

$$\widehat{a}_m = \sum_{l=0}^{N_f-1} a_l \mathbf{w}_m^{N_f H}\mathbf{V}_{\text{eq}}\overline{\mathbf{T}}\mathbf{\Lambda}\mathbf{w}_l^{N_f} + \mathbf{w}_m^{N_f H}\mathbf{V}_{\text{eq}}\widetilde{\eta} \tag{12}$$

for $0 \le m \le N_f - 1$.

If we now design an MMSE equalizer only to combat MCI, then $\mathbf{V}_{\text{eq}}$ is a diagonal matrix with diagonal elements as (see [1, 10])

$$\mathbf{V}_{\text{eq,mmse}}(m,m) = \frac{(\lambda_m)^*}{N_f|\lambda_m|^2 + \sigma^2/(P)}, \quad 0 \le m \le N_f - 1, \tag{13}$$

where $P = E(a_m a_m^*)$ with superscript $*$ denoting complex conjugate. On the other hand, if we choose a ZF equalizer, then the corresponding $\mathbf{V}_{\text{eq}}$ is given by

$$\mathbf{V}_{\text{eq,zf}} = \mathbf{\Lambda}^{-1}. \tag{14}$$

To compute BER with a particular equalizer, we follow the analysis suggested in [6–8]. We decompose the first term of (12) into three parts, a_m^1, a_m^2, and a_m^3, as follows:

$$\widehat{a}_m = a_m^1 + a_m^2 + a_m^3 + \mathbf{w}_m^{N_f H}\mathbf{V}_{\text{eq}}\widetilde{\eta}, \tag{15}$$

where

$$a_m^1 = a_m \mathbf{w}_m^{N_f H}\mathbf{V}_{\text{eq}}\mathbf{E}\mathbf{\Lambda}\mathbf{w}_m^{N_f}, \tag{16}$$

$$a_m^2 = a_m \mathbf{w}_m^{N_f H}\mathbf{V}_{\text{eq}}\left(\overline{\mathbf{T}} - \mathbf{E}\right)\mathbf{\Lambda}\mathbf{w}_m^{N_f}, \tag{17}$$

$$a_m^3 = \sum_{l=0, l\neq m}^{N_f-1} a_l \mathbf{w}_m^{N_f H}\mathbf{V}_{\text{eq}}\overline{\mathbf{T}}\mathbf{\Lambda}\mathbf{w}_l^{N_f}. \tag{18}$$

The matrix $\mathbf{E}$ is a diagonal matrix with its elements as the diagonal elements of $\overline{\mathbf{T}}$. From the structure of $\overline{\mathbf{T}}$ (see (9)), we note that a_m^1 and a_m^2 are the desired symbol multiplied by a real scalar and a complex scalar, respectively, and a_m^3 is the interference from other symbols caused by MCI and

ICI. Though the second term contains the desired symbol, it can add to the first term constructively or destructively because of the associated complex scalar. We, therefore, treat it as the interference and following [7], we define it as self interference. The third term is the interference from other symbols. In view of the assumption that the symbols are identical and independently distributed random variables with zero mean and variance P, and applying the central limit theorem, we model the second and third terms as zero mean and uncorrelated Gaussian variables. The fourth term in (15) is a zero mean Gaussian variable which is uncorrelated with the second and third terms. Further, in view of the i.i.d. nature of the elements of $\widetilde{\eta}$, its variance is independent of which symbol is being decoded.

To find the BER, we first evaluate average SINR for each decoded symbol. Denoting the average SINR for the decoded symbol a_m as SINR_m, we have from (16), (17), (18), and the fourth term in(15)

$$\text{SINR}_m = \frac{E\left(a_m^1 a_m^{1*}\right)}{E\left(a_m^2 a_m^{2*}\right) + E\left(a_m^3 a_m^{3*}\right) + E\left(N_m N_m^*\right)}, \tag{19}$$

where

$$N_m = \mathbf{w}_m^{N_f H} \mathbf{V}_{\text{eq}} \widetilde{\eta}. \tag{20}$$

Assuming that the symbols are drawn from a 4-QAM constellation of average power P and they are equally likely, and the mapping of data bits to symbols is based on Gray encoding, the BER is given by [11]

$$\text{BER} \mid (\mathbf{\Lambda}, \epsilon) \approx \frac{1}{N_f} \sum_{m=0}^{N_f - 1} Q\left(\sqrt{\text{SINR}_m}\right). \tag{21}$$

The above expression can be evaluated using numerical integration for both MMSE and ZF equalizers choosing the corresponding equalizer coefficients in the SINR expression.

4.1. Degradation of MMSE Equalizer Performance at High SNRs. Note that at high SNRs (see (13)),

$$\mathbf{V}_{\text{eq,mmse}}(m,m) \approx \frac{(\lambda_m)^*}{N_f |\lambda_m|^2} = \frac{1}{N_f} \mathbf{V}_{\text{eq,zf}}(m,m). \tag{22}$$

The above relation, combined with the fact that the BER performance of MMSE equalizer is significantly better than that of ZF equalizer at low and moderate SNRs in multipath fading channels (see [1]) and also that ZF performance has a floor at high SNR due to ICI, suggests that the MMSE equalizer performance degrades beyond an SNR value, referred as threshold SNR. This SNR depends on RFO and multipath channel profile. To see if this is the case, we first considered a particular realization of a 6-tap Rayleigh fading channel model [12] and evaluated the BER performance from (21) with both MMSE and ZF equalizers for two values of RFO, 0.05 and 0.03, choosing $N_f = 64$. Figure 3 gives the BER plots which support our above remark regarding the performance of MMSE equalizer. Note from the plots that for RFO = 0.05, the threshold SNR is 28 dB while it is 33 dB for RFO = 0.03. We may point out here that when we considered a particular channel realization in the analysis, we normalized the channel impulse response coefficients to unit-norm. Note that $N_f P$ is the average transmitted signal power in each bin and this prompted us to plot the curves as a function of $N_f P/\sigma^2$.

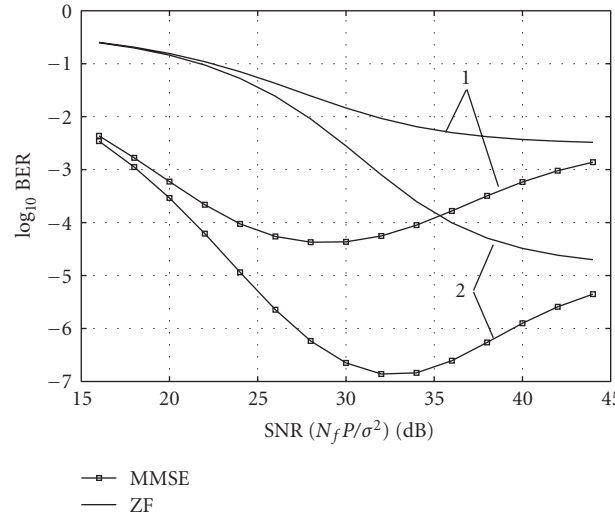

Figure 3: BER performance of MC-CDMA with MMSE and ZF equalizers, evaluated from (21), for RFO = 0.05 (plots marked 1) and RFO = 0.03 (plots marked 2) ($N_f = 64$ and the channel realization is CR-1 given in Table 1, and symbols are from 4-QAM constellation with $P = 1$).

Table 1: $|\lambda_{\max}|/|\lambda_{\min}|$ values for three channel realizations of channel model [12] (CR: channel realization).

	CR-1	CR-2	CR-3
$\lvert\lambda_{\max}\rvert/\lvert\lambda_{\min}\rvert$	114 for $N_f = 64$	67 for $N_f = 64$	17 for $N_f = 64$

Next, we considered 3 different realizations of the same 6-tap channel and Figure 4 shows the BER plots for RFO = 0.05. Note that the degradation happens for the channel realizations with large values of $|\lambda_{\max}|/|\lambda_{\min}|$ (see Table 1) where $|\lambda_{\max}|$ and $|\lambda_{\min}|$ denote, respectively, the largest and smallest of $|\lambda_0|, |\lambda_1|, \ldots, |\lambda_{N_f-1}|$ and correspond to the strongest and weakest bin gains, respectively. Note that the threshold SNR in the case of CR-1 is 28 dB while it is 26 dB for CR-2. We will explain in the next section why the BER performance does not degrade at high SNRs in the case of CR-3.

5. Cause and Remedy for the Degradation

From the results of the preceding section, it is clear that the performance of MC-CDMA with MMSE equalizer degrades beyond a threshold SNR in multipath channels in the presence of RFO. In other words, the SINR decreases with increasing SNR beyond the threshold SNR. We now make an attempt to pinpoint the cause for such behavior.

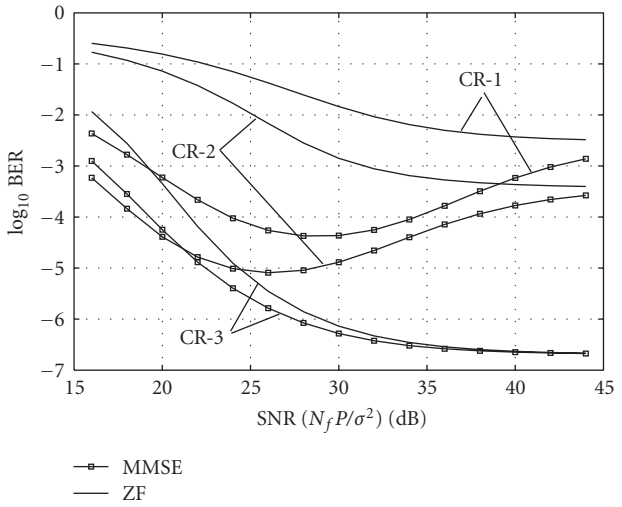

Figure 4: BER performance of MC-CDMA with MMSE and ZF equalizers, evaluated from (21), for three different channel realizations (RFO = 0.05, $N_f = 64$, and CR-1, CR-2, CR-3 refer to the channel realizations given in Table 1, and symbols are from 4-QAM constellation with $P = 1$).

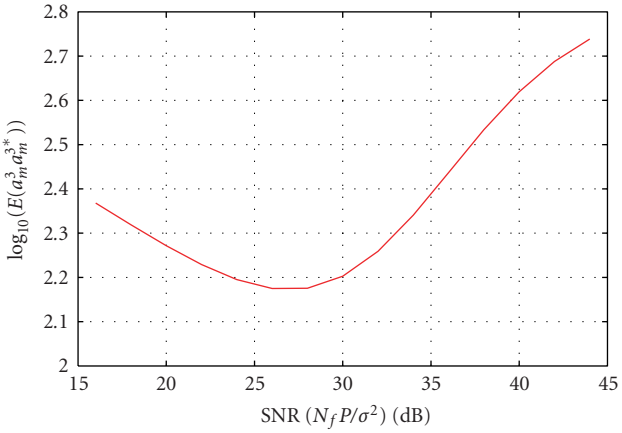

Figure 5: $E(a_{m^3} a_{m^{3*}})$ as a function of SNR for the channel realization CR-1 given in Table 1 ($N_f = 64$ and RFO = 0.05, and symbols are from 4-QAM constellation with $P = 1$).

5.1. Cause. Consider the term a_m^3 (see (18)) contributed by MCI and ICI. We evaluated $E(a_m^3 a_m^{3*})$ as a function of $N_f P/\sigma^2$ with RFO = 0.05 and for CR-1. Note from Figure 5 that the $E(a_m^3 a_m^{3*})$ begins to increase beyond about 28 dB SNR which is the threshold SNR for the plot 1 corresponding to MMSE in Figure 3.

As a_m^3 is the interference from the symbols other than the symbol being decoded and carried by all the subcarriers (see (18)), we express a_m^3 as

$$a_m^3 = \sum_{k=0}^{N_f-1} a_{m,k}^3 \tag{23}$$

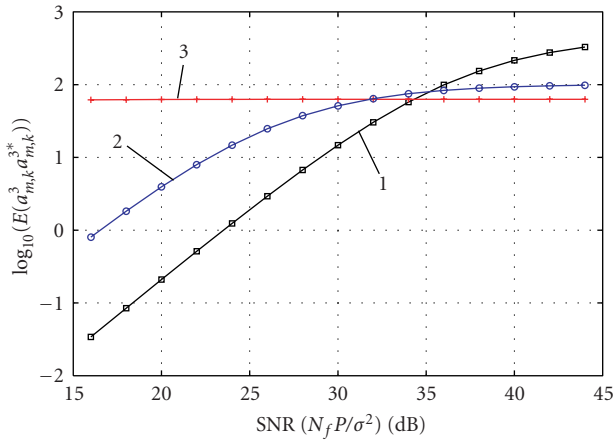

Figure 6: $E(a_{m,k^3} a_{m,k^{3*}})$ as a function of SNR for the channel realization CR-1 given in Table 1 ($N_f = 64$, RFO = 0.05, plot marked 1-weakest bin, plot marked 2-next weakest bin, plot marked 3-strongest bin. Symbols are from 4-QAM constellation with $P = 1$).

with $a_{m,k}^3$ given by

$$a_{m,k}^3 = \sum_{l=0, l\neq m}^{N_f-1} a_l \mathbf{w}_m^{N_f H} \mathbf{V}_{\text{eq,mmse}}^k \overline{\mathbf{T}} \mathbf{\Lambda} \mathbf{w}_l^{N_f}, \tag{24}$$

where

$$\mathbf{V}_{\text{eq,mmse}}^k = \text{diag}\left[0 \ \cdots \ 0 \ \mathbf{V}_{\text{eq,mmse}}(k,k) \ 0 \ \cdots \ 0\right]. \tag{25}$$

Here, $a_{m,k}^3$ represents the amount of interference caused by the symbols other than the symbol being decoded, carried by kth bin. We now examine $a_{m,k}^3$ for three bins: (1) the weakest bin, (2) the next weakest bin, and (3) the strongest bin. Figure 6 gives the plots of $E(a_{m,k}^3 a_{m,k}^{3*})$ for these three bins. We observe the following from the plots.

The interference contribution from the strongest bin (Plot 3) is nearly independent of SNR, while the contribution from the weakest bin (Plot 1) increases monotonically with SNR, tending to a constant value only at very large values of SNR. The contribution from the next weakest bin (Plot 2) increases with SNR initially at a slower rate compared to that in the weakest bin case and tends to a constant value quickly after the SNR exceeds the threshold value 28 dB. This behavior suggests that it is the weakest bin which essentially determines the degradation beyond the threshold SNR.

Now, consider the BER plots of Figure 4 for the case of CR-3. We note from (24) that when k corresponds to the weakest bin, it will have the term $((\lambda_{\min})^*/(N_f|\lambda_{\min}|^2 + \sigma^2/(P)))\lambda_{\max}$. When $\sigma^2/(P)$ is small compared to $N_f|\lambda_{\min}|^2$, we can approximate it to $\lambda_{\max}/N_f\lambda_{\min}$ which suggests that this ratio determines the magnification of interference which is well known. The low value of this ratio for CR-3 (see Table 1) explains why the BER does not degrade as the SNR is increased.

5.2. Remedy. Since the weakest bin essentially determines the degradation, we regularize the corresponding coefficient

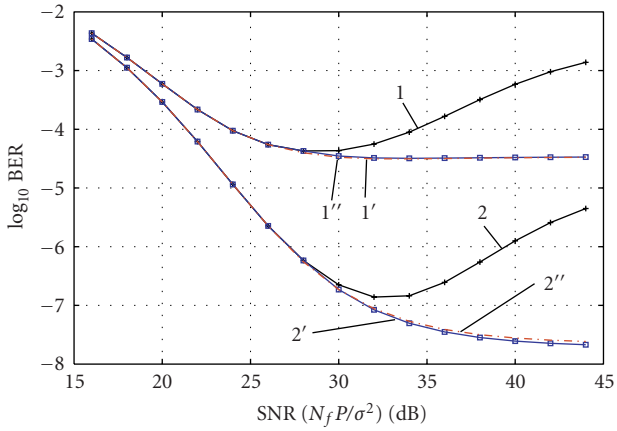

Figure 7: BER performance of MC-CDMA with MMSE equalizer, evaluated using (21) (Plots 1 and 2 are without regularization, plots 1′ and 2′ are with regularization based on the threshold SNR estimated from plot 1 as described in Section 5.3, plots 1′′ and 2′′ are with regularization based on the threshold SNR computed from (26), Plots $(1, 1', 1'')$ and $(2, 2', 2'')$ correspond to RFOs = 0.05 and 0.03, respectively, $N_f = 64$ and channel realization is CR-1 given in Table 1, and symbols are from 4-QAM constellation with $P = 1$).

of the equalizer, that is, $\mathbf{V}_{\text{eq,mmse}}(k,k)$, k corresponding to $\lambda_{\min}$, as $(\lambda_{\min})^*/(N_f(|\lambda_{\min}|^2 + (\sigma^2/N_fP)_{\text{th}}))$ and use the regularized equalizer for the SNRs exceeding the threshold value. Here, $(\sigma^2/N_fP)_{\text{th}}$ denotes the value of (σ^2/N_fP) at the threshold SNR. This implicitly assumes that we have the knowledge of the threshold SNR. Before addressing this issue, we first examine if the suggested regularization prevents the degradation. Figure 7 gives the BER plots for CR-1 with equalizer coefficients (13) (Plot 1) and with the regularization as suggested above (Plot 1′). In this figure, we chose the value of RFO as 0.05 and $N_f = 64$ and applied the regularization with $(\sigma^2/N_fP)_{\text{th}}$ corresponding to the threshold SNR 28 dB. Note that the regularization prevents the degradation.

Use of above threshold SNR implicitly assumes that we have the knowledge of RFO value. In practice, it will not be the case. However, from the system specifications and the synchronization algorithm, one will have an estimate of the maximum possible RFO which is of the order 10^{-2}. It will then be of interest to know how the regularization, computed based on the assumed knowledge of maximum RFO value, will perform if the actual RFO is different from the assumed. In Figure 7, Plots 2 and 2′ correspond to the equalizer (13) and the regularized equalizer, respectively, for RFO = 0.03. We note that the suggested regularization prevents the degradation even though the actual RFO is different from the assumed value based on which the threshold SNR and the regularized coefficient were computed. From these results, we are tempted to state that the knowledge of the actual value of RFO is not critical to the suggested method.

5.3. Estimating the Threshold SNR. From the estimated channel impulse response coefficients, we compute λ_k's. Assuming a maximum value for RFO, and for a given transmitted symbol constellation, we can evaluate BER as a function of (N_fP/σ^2) using (21). Evaluate the BER over a range of SNR values with a spacing of 2 dB, determine the SNR at which the BER starts increasing and take the immediate previous SNR value as the estimate of the threshold SNR $(N_fP/\sigma^2)_{\text{th}}$.

5.4. An Approximate Value of Threshold SNR. Recall that in arriving at the regularization coefficient, we assumed (σ^2/P) to be small compared to $N_f|\lambda_{\min}|^2$ and argued that major contribution to the term a_m^3 comes from the weakest bin if $|\lambda_{\max}|/|\lambda_{\min}|$ is large. This suggests that an approximate value of the threshold SNR can be obtained from

$$\left(\frac{N_fP}{\sigma^2}\right)_{\text{th-approx}} = \frac{3}{|\lambda_{\min}|^2}. \tag{26}$$

For CR-1, (26) gives nearly 23 dB. Note that only the knowledge of CSI is required in this case. To see how the regularization based on the approximate threshold SNR performs, we computed this from (26) and regularized the equalizer coefficient corresponding to the weakest bin as $(\lambda_{\min})^*/(N_f(|\lambda_{\min}|^2 + (\sigma^2/N_fP)_{\text{th-approx}}))$ and evaluated the corresponding BER using (21). Plots 1′′ and 2′′ of Figure 7 show these results.

The regularization based on the approximate value of the threshold SNR prevents degradation independent of RFO value and spread in the bin gains. However, at higher SNRs, there is a small loss in the performance compared to that based on better estimate of the threshold SNR computed as described in the previous section. In the next section, we present results for $N_f = 16$ and 256 to show the effectiveness of the approximate threshold SNR.

6. Simulation Results

To see how the proposed regularization performs in multipath Rayleigh fading channels, we conducted simulations using the following simulation setup.

We considered a burst communication in slow fading scenario. Here, we assume perfect timing and channel estimate, and assume a maximum value of RFO as 0.05. We considered 10^6 realizations of the channel model given in [12], normalizing each tap variance such that the total variance is one. This results in the average received signal power in each bin same as the transmitted power which is N_fP. Thus, the N_fP/σ^2 represents the received SNR in each bin. The data burst consists of 100 OFDM symbols where each OFDM symbol is made up of N_f 4-QAM symbols and mapping of data bits to symbols is based on Gray encoding. A complex Gaussian noise, with appropriate variance to give the required SNR, is added to the received signal. The noise corrupted received signal is preprocessed with (i) MMSE equalizer (13), (ii) regularized equalizer based on threshold SNR estimated as described in Section 5.3,and (iii) regularized equalizer based on the approximate threshold SNR computed from (26). In each case, for different values of N_fP/σ^2, the preprocessed received signal is decoded and the number of decoded symbols in error is noted. This is repeated for 10^6 channel realizations, choosing a different

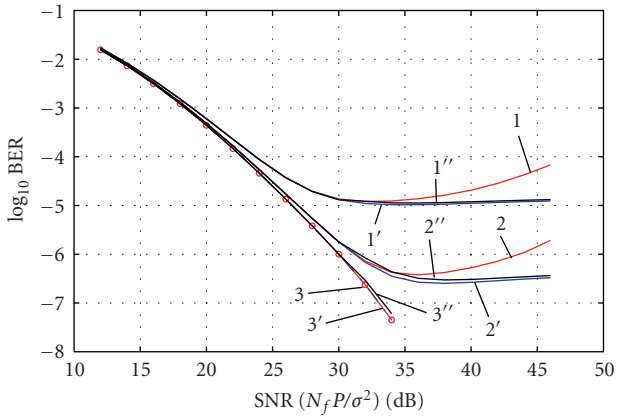

FIGURE 8: BER performance of MC-CDMA for $N_f = 64$ with MMSE equalizer, averaged over 10^6 realizations of the channel model given in [12] with tap variances normalized such that the total variance is one (Plots 1, 2, 3 are without regularization, $1', 2', 3'$ are with regularization based on the threshold SNR estimated as given in Section 5.3 with RFO = 0.05, plots $1'', 2'', 3''$ are with regularization based on the threshold SNR computed from (26), plots $(1, 1', 1'')$, $(2, 2', 2'')$, and $(3, 3', 3'')$ correspond to RFOs = 0.05, 0.03 and 0.01, respectively, and symbols are from 4-QAM constellation with $P = 1$).

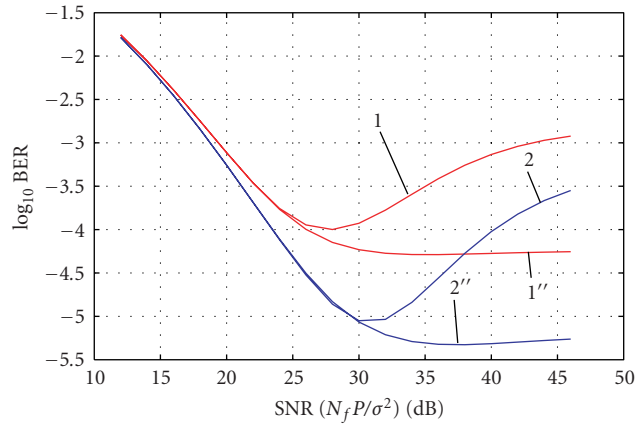

FIGURE 9: BER performance of MC-CDMA for $N_f = 16$ with MMSE equalizer, averaged over 10^6 realizations of the channel model given in [12] with tap variances normalized such that the total variance is one (Plots 1, 2 are without regularization, plots $1'', 2''$ are with regularization based on the threshold SNR computed from (26), plots $(1, 1'')$, $(2, 2'')$ correspond to RFOs = 0.05 and 0.03, respectively, and symbols are from 4-QAM constellation with $P = 1$).

sequence of transmitted 4-QAM symbols and a different noise sequence in each case, and the number of decoded symbols in error is noted. From the results so obtained, the average symbol error probability is computed for each value of $N_f P/\sigma^2$, and one half of this is taken as the BER.

We first considered $N_f = 64$. For each realization, we computed λ_k's and regularized the equalizer coefficient corresponding to the weakest bin for every realization with $|\lambda_{\max}|/|\lambda_{\min}| \geq 64$, using two different values of threshold SNR as described above, and processed the noise corrupted received signal. The results of BER are given in Figure 8. We note from the plots that the suggested regularization performs as predicted. Further, the regularization with approximate threshold SNR performs nearly as good as that with better estimate of the threshold SNR over a wide range of RFO values (0.01 to 0.05). This is very significant since the approximate threshold SNR is computed from the knowledge of CSI only, which is available at the receiver.

To verify if regularization with approximate threshold SNR performs well for other values of N_f, we considered $N_f = 16$ and 256 and used the same simulation setup as given above.

6.1. $N_f = 16$. In this case, we regularized the equalizer coefficient corresponding to weakest bin, using the threshold SNR computed from (26), for every realization with $|\lambda_{\max}|/|\lambda_{\min}| \geq 16$. The results are shown in Figure 9. The plots show that the regularization based on approximate threshold SNR performs well.

6.2. $N_f = 256$. In this case, it has been observed from the simulations that with regularized equalizer coefficients

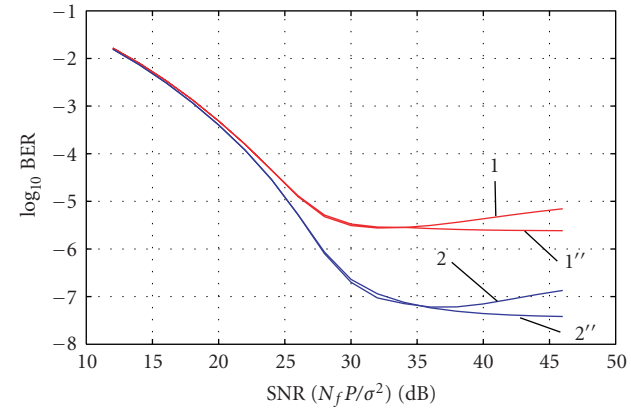

FIGURE 10: BER performance of MC-CDMA for $N_f = 256$ with MMSE equalizer, averaged over 10^6 realizations of the channel model given in [12] with tap variances normalized such that the total variance is one (Plots 1, 2 are without regularization, plots $1'', 2''$ are with regularization corresponding to the 5 bins whose gains are least of the 256 bin gains, computing the threshold SNR from (26) by replacing $\lambda_{\min}$ with the corresponding bin gain, plots $(1, 1'')$, $(2, 2'')$ correspond to RFOs = 0.05 and 0.03, respectively, and symbols are from 4-QAM constellation with $P = 1$).

corresponding to 5 bins whose gains are least of the 256 λ_k's, choosing the the threshold SNR from (26) replacing $\lambda_{\min}$ with λ_k of the corresponding bin, the degradation can be prevented. We applied this for every realization with $|\lambda_{\max}|/|\lambda_{\min}| \geq 128$ and the results are given in Figure 10. Note that with regularization using the approximate threshold SNR, the BER reaches a floor instead of rising.

7. Conclusions

In this paper, we have studied the BER performance of MC-CDMA with MMSE equalizer in the presence of RFO in multipath Rayleigh fading channels and brought out the threshold effect; that is, beyond certain SNR the BER deteriorates, and the value of this SNR depends on the value of RFO and the channel profile. An attempt has been made to pinpoint the cause for such behavior and regularization of the equalizer coefficient(s) has been suggested to prevent the degradation. The regularization requires knowledge of the threshold SNR. We have shown with numerical and simulation results that with an approximate threshold SNR, which can be computed from the knowledge of CSI only, the degradation can be prevented.

Acknowledgments

The authors gratefully acknowledge the useful comments and suggestions of the reviewers which improved the clarity of the paper. This work is partly supported by CR Rao Advanced Institute of Mathematics, Statistics and Computer Science.

References

[1] K. Fazel and S. Kaiser, *Multi-Carrier and Spread Spectrum Systems*, Wiley Series, John Wiley & Sons, New York, NY, USA, 2003.

[2] M. Speth, S. A. Fechtel, G. Fock, and H. Meyr, "Optimum receiver design for wireless broad-band systems using OFDM-part I," *IEEE Transactions on Communications*, vol. 47, no. 11, pp. 1668–1677, 1999.

[3] Ch. N. Kishore and V. U. Reddy, "A frame synchronization and frequency offset estimation algorithm for OFDM system and its analysis," *EURASIP Journal on Wireless Communications and Networking*, vol. 2006, Article ID 57018, 16 pages, 2006.

[4] T. M. Schmidl and D. C. Cox, "Robust frequency and timing synchronization for OFDM," *IEEE Transactions on Communications*, vol. 45, no. 12, pp. 1613–1621, 1997.

[5] L. Rugini and P. Banelli, "BER of OFDM systems impaired by carrier frequency offset in multipath fading channels," *IEEE Transactions on Wireless Communications*, vol. 4, no. 5, pp. 2279–2288, 2005.

[6] Y. Kim, S. Choi, C. You, and D. Hong, "BER computation of an MC-CDMA system with carrier frequency offset," in *Proceedings of IEEE International Conference on Acoustics, Speech and Signal Processing (ICASSP '99)*, vol. 5, pp. 2555–2558, Phoenix, Ariz, USA, March 1999.

[7] J. Jang and K. B. Lee, "Effects of frequency offset on MC/CDMA system performance," *IEEE Communications Letters*, vol. 3, no. 7, pp. 196–198, 1999.

[8] Y. Nasser, M. des Noes, L. Ros, and G. Jourdain, "Sensitivity of multicarrier two-dimensional spreading schemes to synchronization errors," *EURASIP Journal on Wireless Communications and Networking*, vol. 2008, Article ID 561869, 16 pages, 2008.

[9] T. Pollet, M. Van Bladel, and M. Moeneclaey, "BER sensitivity of OFDM systems to carrier frequency offset and Wiener phase noise," *IEEE Transactions on Communications*, vol. 43, no. 234, pp. 191–193, 1995.

[10] N. Yee and J.-P. Linnartz, "Wiener filtering of multi-carrier CDMA in a Rayleigh fading channel," in *Proceedings of the 5th IEEE International Symposium on Personal, Indoor and Mobile Radio Communications (PIMRC '94)*, The Hague, The Netherlands, September 1994.

[11] J. Proakis, *Digital Communications*, McGraw-Hill, New York, NY, USA, 3rd edition, 1995.

[12] K. Pahlavan and A. H. Levesque, *Wireless Information Networks*, Wiley InterScience, New York, NY, USA, 2nd edition, 2005.

Preliminary call for papers

The 2011 European Signal Processing Conference (EUSIPCO-2011) is the nineteenth in a series of conferences promoted by the European Association for Signal Processing (EURASIP, www.eurasip.org). This year edition will take place in Barcelona, capital city of Catalonia (Spain), and will be jointly organized by the Centre Tecnològic de Telecomunicacions de Catalunya (CTTC) and the Universitat Politècnica de Catalunya (UPC).

EUSIPCO-2011 will focus on key aspects of signal processing theory and applications as listed below. Acceptance of submissions will be based on quality, relevance and originality. Accepted papers will be published in the EUSIPCO proceedings and presented during the conference. Paper submissions, proposals for tutorials and proposals for special sessions are invited in, but not limited to, the following areas of interest.

Areas of Interest

- Audio and electro-acoustics.
- Design, implementation, and applications of signal processing systems.
- Multimedia signal processing and coding.
- Image and multidimensional signal processing.
- Signal detection and estimation.
- Sensor array and multi-channel signal processing.
- Sensor fusion in networked systems.
- Signal processing for communications.
- Medical imaging and image analysis.
- Non-stationary, non-linear and non-Gaussian signal processing.

Submissions

Procedures to submit a paper and proposals for special sessions and tutorials will be detailed at www.eusipco2011.org. Submitted papers must be camera-ready, no more than 5 pages long, and conforming to the standard specified on the EUSIPCO 2011 web site. First authors who are registered students can participate in the best student paper competition.

Important Deadlines:

Proposals for special sessions	15 Dec 2010
Proposals for tutorials	18 Feb 2011
Electronic submission of full papers	**21 Feb 2011**
Notification of acceptance	23 May 2011
Submission of camera-ready papers	6 Jun 2011

Webpage: www.eusipco2011.org

Organizing Committee

Honorary Chair
Miguel A. Lagunas (CTTC)

General Chair
Ana I. Pérez-Neira (UPC)

General Vice-Chair
Carles Antón-Haro (CTTC)

Technical Program Chair
Xavier Mestre (CTTC)

Technical Program Co-Chairs
Javier Hernando (UPC)
Montserrat Pardàs (UPC)

Plenary Talks
Ferran Marqués (UPC)
Yonina Eldar (Technion)

Special Sessions
Ignacio Santamaría (Unversidad de Cantabria)
Mats Bengtsson (KTH)

Finances
Montserrat Nájar (UPC)

Tutorials
Daniel P. Palomar (Hong Kong UST)
Beatrice Pesquet-Popescu (ENST)

Publicity
Stephan Pfletschinger (CTTC)
Mònica Navarro (CTTC)

Publications
Antonio Pascual (UPC)
Carles Fernández (CTTC)

Industrial Liaison & Exhibits
Angeliki Alexiou (University of Piraeus)
Albert Sitjà (CTTC)

International Liaison
Ju Liu (Shandong University-China)
Jinhong Yuan (UNSW-Australia)
Tamas Sziranyi (SZTAKI -Hungary)
Rich Stern (CMU-USA)
Ricardo L. de Queiroz (UNB-Brazil)